Journal of Clinical Periodontology
Official Journal of The European Federation of Periodontology
Founded by the British, Dutch, French, German, Scandinavian, and Swiss Societies of Periodontology

J Clin Periodontol 2009; 36: 598–603 doi: 10.1111/j.1600-051X.2009.01429.x

Macro- and micro-anatomical, histological and computed tomography scan characterization of the nasopalatine canal

Xin Liang[1,2], Reinhilde Jacobs[1], Wendy Martens[3], YuQian Hu[1], Peter Adriaensens[4], Marc Quirynen[5] and Ivo Lambrichts[3]

[1]Oral Imaging Centre, Faculty of Medicine, School of Dentistry, Katholieke Universiteit Leuven, Leuven, Belgium; [2]College of Stomatology, Dalian Medical University, Liaoning, China; [3]Department of Medical Basic Sciences, Faculty of Medicine, University of Hasselt, Diepenbeek, Belgium; [4]Department of Applied Chemistry, University of Hasselt, Diepenbeek, Belgium; [5]Department of Periodontology, Faculty of Medicine, Katholieke Universiteit Leuven, Leuven, Belgium

Liang X, Jacobs R, Martens W, Hu YQ, Adriaensens P, Quirynen M, Lambrichts I. Macro- and micro-anatomical, histological and computed tomography scan characterization of the nasopalatine canal. J Clin Periodontol 2009; 36: 598–603. doi: 10.1111/j.1600-051X.2009.01429.x.

Abstract

Aim: To determine the human anatomic variability of the nasopalatine canal and determine its characteristics using an anatomical, histological and computed tomography (CT) scan evaluation.

Materials and Methods: Measurements for the canal characteristics were carried out on 163 dry human skulls and 120 upper jaw spiral CT scans, taken from patients for pre-operative planning purposes of implant placement in the incisor region. Furthermore, four human cadaver specimens were imaged using a high-resolution magnetic resonance imaging (HR-MRI) unit. Afterwards, these specimens were serially sectioned for histological examination to evaluate the nasopalatine canal region and its content.

Results: The nasopalatine canal anatomy showed a large variability in morphology and dimensions, with the canal branching in up to four canals at the level of the nose. The canal diameter was on average 3.3 mm ($\pm$ 0.9 mm SD), and typically enlarged by age and male gender ($p < 0.05$). HR-MRI and histological sections enabled to identify the neurovascular structures within the canals.

Conclusions: The large anatomic variations, the increased canal dimensions with age and the neurovascular canal content are all factors favouring a thorough three-dimensional planning before surgery, such as implant placement, of the anterior maxillary region.

Key words: anatomy; histology; HR-MRI; nasopalatine canal; spiral-CT

Accepted for publication 17 April 2009

It is important to consider the presence of the nasopalatine canal and evaluate its morphology and dimensions before surgical procedures e.g. implant surgery or anaesthesia.

Knowing the location of the nasopalatine canal and its content, is important during surgical procedures like implant placement. Contact of dental implants with nervous tissue may cause non-osseointegration of the implant or lead to sensory dysfunction (Artzi et al. 2000, Casado et al. 2008). The nasopalatine canal commences towards the front of the floor of each nasal cavity. Each canal opens into the midline incisive foramen on the median plane of the palatine process of the maxilla, posterior to the central incisors and transmits nasopalatine vessels and nerves, branches of the maxillary division of the trigeminal nerve and the maxillary artery. The nasopalatine canal exists of one, two or multiple canals (Mraiwa et al. 2004, White & Pharoah 2004).

Trauma and pathology of the nasopalatine canal region were dealt with in some previous reports (Swanson et al. 1991, Kreidler et al. 1993, Daley et al. 1994). The anterior maxilla region is being referred by the former report as the ''traumatic zone'' (Tolstunov 2007); Daley et al. (1994) found 73% of 295

Conflict of interest and source of funding statement

The study has no special source of funding. None of the above author or author's institution has conflicts of interests.

cases involving nonodontogenic tumors were nasopalatine duct cysts. Yet there are poorly documented anatomical variations in dimensions and morphology of this canal (Chandler & Gray 1996, Jacob et al. 2000, Moss et al. 2000). Though, with the increasing demand for rehabilitation of the edentulous maxilla by means of osseointegrated implants, pre-operative evaluation of the nasopalatine canal region has regained attention (Kraut & Boyden 1998, Cavalcanti et al. 1999, Artzi et al. 2000). Kraut & Boyden (1998) describe the difficulties and anatomic limitations regarding the location of the nasopalatine canal in relation to maxillary central incisor implants. Ninety-six percentage of the patients in their study had volumetric relationships between this canal and the maxillary central incisors, which would not preclude ideal placement of implants in the sockets of the maxillary central incisors. After tooth loss, the atrophy of disuse may influence the surrounding structures. The nasopalatine canal may enlarge and the neurovascular bundles inside may ultimately emerge from the ridge crest (Mardinger et al. 2008). Both pathological symptoms and morphological variation or change of the nasopalatine canal may remain a complex restorative challenge. Indeed, before carrying out a surgical procedure in the anterior jaw bones in both upper and lower jaws, it is of utmost importance to consider and precisely locate the presence of neurovascular bundles. Jacobs et al. (2007) first reported that the use of high-resolution magnetic resonance imaging (HR-MRI) for micro-anatomical observations of jaw bone neurovascularization can provide new insights and give clear answers to the ongoing debates. Whenever a true neurovascular bundle would be identified in this region and considered to be functional, surgery might not be without risks.

The characteristic description of the nasopalatine canal and the knowledge on its content and variable appearance are crucial to optimize surgical planning and avoid complications in this aesthetically demanding region. Indeed, tooth loss in the central incisor region may often be caused by trauma. The inherent direct bone loss caused by this together with the indirect bone loss induced by nasopalatine canal expansion after tooth extraction (Mardinger et al. 2008) may compromise an optimal aesthetic result. The introduction of 3D-cone beam computed tomography (CT) and its potentials for 3D CT-based surgical planning and transfer are advantageous striving to the best treatment strategy while considering the nasopalatine canal. It is essential to obtain thorough knowledge on anatomical appearances and variation and to describe visualization on spiral CT images taken for pre-operative planning purposes (Mraiwa et al. 2004).

The aim of this study was to determine the human anatomic variability of the nasopalatine canal and determine its characteristics using an anatomical, histological and CT scan evaluation.

Materials and Methods

Four human maxillary jaw bone specimens from formalin-perfused cadavers and 163 dry Indian human skulls were obtained with ethical approval by the Institute for Biomedical Research (BIOMED of University Center Hasselt, Belgium).

The study included also 120 upper jaw spiral CT scans, taken from patients (16–73 years old; 65 females) for pre-operative planning purposes of implant placement in the incisor region (Department of Periodontology, University Hospital, Katholieke Universiteit Leuven, Belgium).

Macroanatomical assessment

Measurements of the size and location of the nasopalatine canal were carried out on 163 dry human skulls. The diameter of both foramina was measured at the entrance of the bony canal. The location of the nasopalatine foramen was determined as the distance of the canal to the marginal bone crest at the level of the incisor teeth.

Micro-anatomical assessment

The contents of the nasopalatine canal obtained from four formaline-fixed human cadavers were dissected and additionally analysed using HR-MRI (Varian®, Nuclear Magnetic Resonance Instruments, Palo Alto, CA, USA). This Varian Unity 400 spectrometer operated at 9.4 T and was equipped with an imaging probe with a 25-mm diameter. For the coronal and transversal views of the anterior maxilla, 1-mm sections were selected with a field of view of $25/30 \times 25$ mm and a data acquisition matrix of $500/600 \times 500$ pixels. The corresponding spatial resolution was $50 \times 50\,\mu$m. Acquisition parameters were put at 2500/15–17 ms (TR/TE) producing essentially concentration images. The total acquisition time was 17 h. These HR-MRI images were compared with histological and dissection images of the same specimen.

Histological assessment

The content was histologically characterized after decalcification in 5% nitric acid (HNO_3) during 2 months and routine paraffin embedding during 24 h afterwards. Serial 7 μm sections were cut with the microtome. After standard histological staining procedures with the Trichrome of Masson staining, slices were analysed using the Eclipsenet and SIS® image analysis software (SIS-Soft-Imaging, Muenster, Germany).

Radiographic assessment

The study material included 120 skull spiral CT scans (Somatom plus S®; Siemens, Erlangen, Germany), taken from patients (16–73 years old; 65 females) for pre-operative planning purposes of bilateral implant placement in the maxilla incisor region. All patients had given their informed consent for the CT while consulting the Department of Periodontology of the University Hospitals (K. U. Leuven). The group was divided into a dentate anterior maxilla group ($n = 60$) and an edentulous maxilla group ($n = 60$).

All CT scans were taken using a standard exposure and patient positioning protocol. This included around 39 axial CT scan slices with a slice thickness of 1 mm and exposure setting of 120 kV; 165/85 mA. The window was set between 2500 and 3000 and the centre was usually set at 500. Reformatted cross-sectional images, taken 2 mm apart from each other, were obtained through the Dental CT® software (Siemens).

Basic observations included the number of canals, their respective anatomical location and morphological variations. All axial, panoramic, and reformatted cross-sectional images were carefully examined under standardized viewing conditions (masked viewing box in a light-dimmed room). Furthermore, linear measurements were performed using a Mitutoyo® digital sliding calliper (Mitutoyo, Andover, UK, accuracy 0.01 mm) to describe the foramina and canal characteristics, including the canal diameter, the length and slope with the horizontal plate, the vertical slice of the palate bone and the incisor tooth (Fig. 1). Two observers (specialists working at the oral

imaging centre, K. U. Leuven) assessed the morphology and canal dimensions using an interactive viewing of 3D CT images. One month later, 20% of the measurements of the 120 cases were repeated to check and intra- and inter-observer variability.

Data and statistical analysis

All data were gathered, and statistically analysed by means of Statistica for Windows® Software Version 5.1 (Stat Soft, Tulsa, OK, USA). A 5% level of significance was chosen. Simple regression analysis was applied to find out influence of age on diameter and length of the whole group; ANOVA (analysis of variance) design was used to describe the influence of gender, dental status and canal morphology on dimensional characteristics.

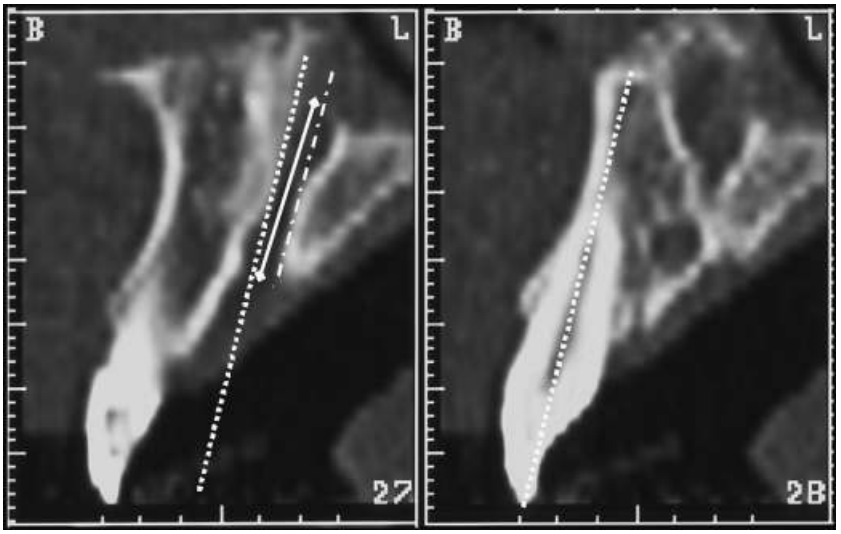

Fig. 1. Drawing shows the measurements on the cross sections of the spiral computed tomography images (◆⟷◆: length of the canal; ◆⟷◆ *versus* – · – : angle between the canal and the palate; ◆⟷◆ *versus* ▪▪▪▪▪: angle between the canal and the tooth axis).

Results

Macroanatomical assessment

The size of the foramen at the entrance of the bony canal and the location of the foramen to the marginal bone crest at the level of the incisors were both measured on 163 dry human skulls (Table 1). The nasopalatine foramen had a mean coronal size of 3.4 mm (± 0.9 mm SD). The distance of the foramen to the marginal bone crest had an average of 9.4 mm (± 2.1 mm SD). The shape of the canal was conical or cylindrical: Out of the 163 dry samples, 75 were classified as cone-shape cases while 87 were described as cylindrical. The cone shape was found in small canals (< 3 mm) in contrast to the cylindrical ones (> 4 mm) (Table 2).

Table 1. Size and location of the nasopalatine foramen in the ex vivo study

	n	Mean (mm)	SD (mm)
Coronal size	163	3.4	0.9
Distance	163	9.4	2.1

SD, standard deviation.

Table 2. The proportion of two shape types of nasopalatine canal related to diameter size in the ex vivo study

	< 4 mm (%)	> 4 mm (%)	< 3 mm (%)	> 3 mm (%)
Cone	57.4	21.9	72.7	33.0
Cylinder	42.6	78.1	27.3	67.0

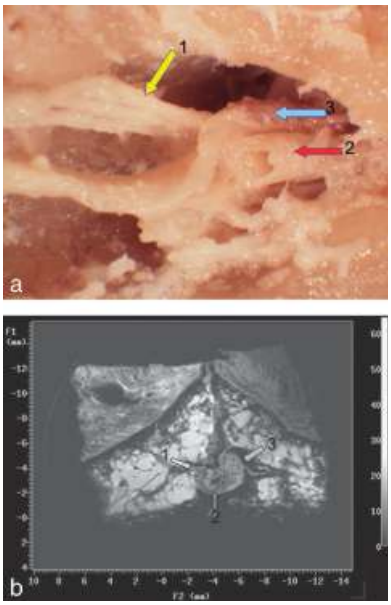

Fig. 2. A dissection image (2a) matched with high-resolution magnetic resonance imaging image (2b), both showing the branches of the maxillary division of the trigeminal nerve (arrow 1), the maxillary artery (arrow 2) and the vein (arrow 3) forming the neurovascular bundle of the nasopalatine canal.

Micro-anatomical and histological assessments

Branches of the maxillary division of the trigeminal nerve and the maxillary artery running through the nasopalatine canal were found by dissection (Fig. 2a). HR-MRI images could visualize the neurovascular bundle contained in the nasopalatine canal very well. On the coronal section, there was a little white triangle (Fig. 2b) indicating that the artery was lying in an anterior canal. On transversal HR-MRI images (Fig. 3a), neurovascular bundles of the nasopalatine canal and the palatine suture were identified, and these were confirmed by the matching histological images (Fig. 3b). The two separate canals were most likely the Stenson canals, each containing the nasopalatine nerve and terminal branches of the descending palatine artery (Fig. 4). The nasopalatine canal contained a large artery surrounded by veins and myelinated nerves, with the myelinated nerve bundle most probably being the nasopalatine nerve. Seromucus glands were also observed (Fig. 5).

Radiographic assessment

On spiral CT scans, nasopalatine canals were branching in up to four canals while travelling from the palate to the nose level. One canal was detected in 53 cases (44%), in 47 cases two canals were noted (39%), in another 20 cases (17%), three or four canals were noted (Fig. 6) (Table 3). The mean (± SD) diameter of the canal structures in this clinical dataset was 3.6 (± 1.0) mm, respectively, with an average length of 9.9 (± 2.6) mm. The canal was located on average 77.4° (± 8.9°) to the horizontal plate. The slope between canal and vertical slice of the palate bone was on average 4.9° (± 5.4°). The slope between canal and incisor tooth was on

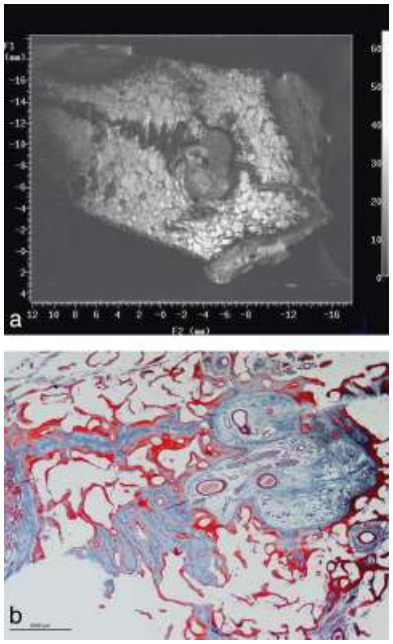

Fig. 3. Matching magnetic resonance imaging image (3a) with the histological image (3b). Both images show the content of the nasopalatine canal and the maxillary suture.

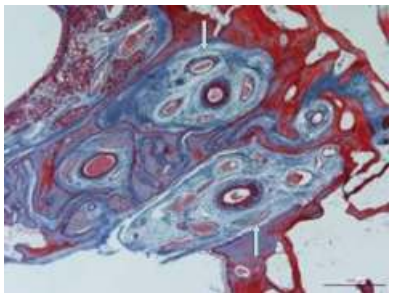

Fig. 4. Histological section shows that the nasopalatine canal is branching in the foramina of Stenson (arrows), both containing neurovascular bundles.

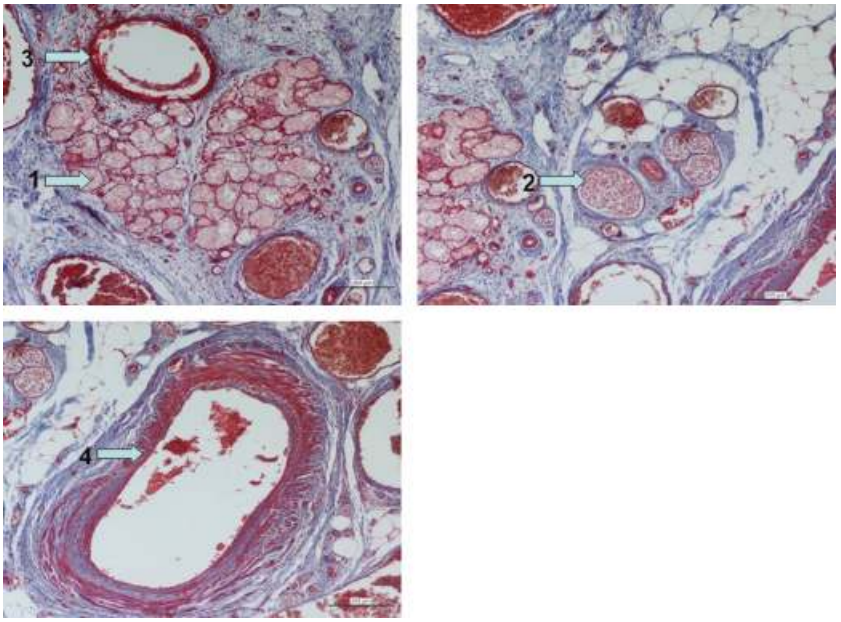

Fig. 5. Light microscopic images show the contents of the nasopalatine canal: seromucus glands (arrow 1), myelinated nerve tissue (arrow 2), veins (arrow 3) and a central artery (arrow 4).

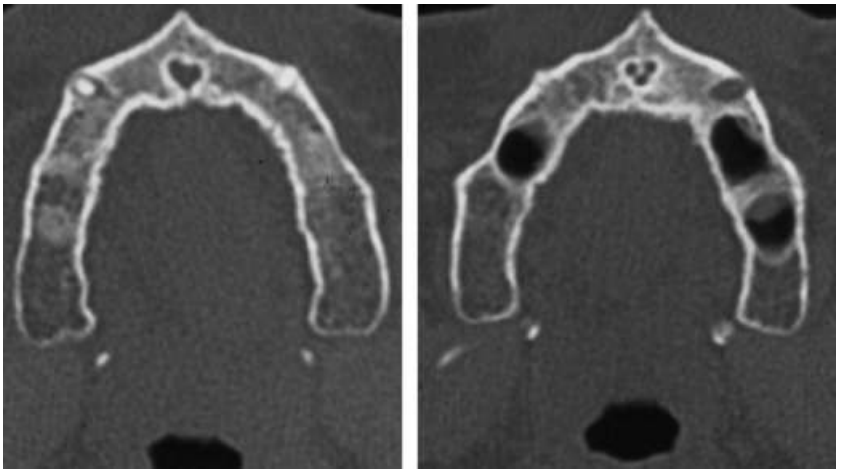

Fig. 6. Axis images from spiral computed tomography scanner show the cone shaped canal running into three canals in the nasal floor.

average 7.9° (± 5.7°) (Table 4). Intra-observer variability was expressed by the coefficient of variation (CV%) and generally below 2%. Inter-examiner variability showed a variability of 5% or lower.

Linear regression analysis showed a significant difference between age and canal diameter ($p = 0.04$). The diameter had a trend towards enlargement when people got older (Fig. 7), and those elderly were more often edentulous ($p = 0.005$). But the present study did not find a significant difference ($p = 0.7$) between the diameter of the edentulous group (3.6 mm) and the dentate group (3.5 mm). The canal was significantly longer in the dentate group (10.6 mm) than the edentulous group (9.2 mm) ($p = 0.003$). Significant gender differences were noted, with males having significantly longer ($p = 0.000001$) and wider canals ($p = 0.05$). Other relationship tests were not found to be significant.

Table 3. The distribution of the number of canals running into the nasal floor in the ex vivo study

Number of canals on the nasal level	Number of cases	%
1 canal	53	44
2 canals	47	39
3 or 4 canals	20	17

Discussion

The use of implants in the incisor region of upper jaw has become part of routine practice of dentistry (Haas et al. 1996, Higginbottom & Wilson 1996), but the location and variability of the nasopalatine canal may hamper this treatment (Kraut & Boyden 1998, Mraiwa et al. 2004). Kraut & Boyden (1998) reported that a nasopalatine canal of a size that will be detrimental to the placement of dental implants is approximately 4%. When the nasoplatine canal is used for implant surgery, usually the canal is filled up with bone grafting material

Table 4. Dimensional measurements of the nasopalatine canal, assessed on a clinical CT dataset

	n	Mean
Diameter	120	3.6 mm
Length	120	9.9 mm
Angle 1 (with horizontal plate)	120	77.4°
Angle 2 (with palate bone margin)	120	4.9°
Angle 3 (with incisor tooth)	120	7.9°

CT, computed tomography.

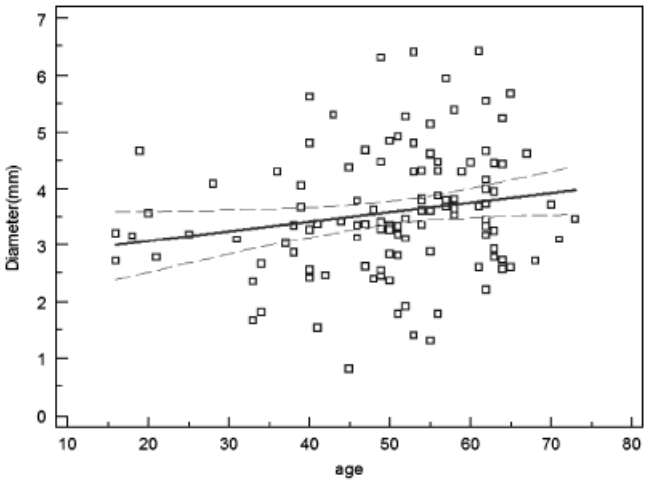

Fig. 7. The graphic shows the regression confidence between age and canal diameter.

after having curetted the complete soft tissue content with removal of all neurovascular tissues from the foramen (Rosenquist & Nyström 1992, Scher 1994). A ''configurated cortico-cancellous block'' technique was introduced by Artzi et al. (2000). With this technique, the block graft pushes soft tissue content (nasopalatine nerve and vessels) posteriorly, as such that the nerve and vessels are clinically preserved and unharmed. Without any further complications or sensory disturbances, the successful displacement enables implants to achieve maximum osseointegration in the post-surgical healing phase.

The nasopalatine branches are the sutures which originate from the fusion of the primary and secondary palatal plates (Radlanski et al. 2004). In the present study, four formalin-fixated specimens were successfully examined using HR-MRI unit. The results were confirmed by histology and micro-anatomical dissection for determining the content of the nasopalatine canal. Regarding the branches of the nasopalatine canal sprouting to the left and right, placing an implant to the left or right of the canal was considered risky. Sicher & DuBrul (1975) described the anterior palatine artery as running forwards in a groove between the horizontal palatine process of the maxilla and the inner plate of the alveolar process, giving numerous branches medially and laterally with the terminal branch reaching the incisive foramen. To avoid disturbing the neurovascular bundles and causing any complication, this important dimensional variability should be taken into account when dealing with surgical procedures. Hassanali & Mwaniki (1984) measured Kenyan skulls and found an average frontal diameter of 3.5 mm. They reported that the diameter of the cone shaped canal is mostly <4 mm, but the diameter of the cylindrical canal >4 mm, which was found in the present study too. However, more cone shaped canals were found in the Kenyan skull study. This difference may be caused by different study samples. In the present study, Indian skulls were used.

Measurements of the nasopalatine canal region on 2D reformatted spiral CT are accurate and not significantly different from direct measurements on cadaver skulls (Cavalcanti et al. 1999). In the present study, the skull measurements cannot really be compared with the spiral CT measurements because of the two different sample races. Mraiwa et al. (2004) pointed out the variability both regarding the dimensions and the morphological appearance of the nasopalatine canal. Most variation occurred at the level of the nasal floor. Sicher (1962) reported that nasopalatine foramina might be present from a single up to six separate foramina. In contrast, in our study, up to four foramina were found, in only 1% of the cases.

In the present spiral CT study, there were some dimensional variabilities related to the samples' age, gender and dental status. The canal diameter enlarged with age. But as the number of edentulous cases was also significantly increased by age, the enlarged diameter might also be caused by edentulism and bone resorption, even if there was no obvious significant difference on the canal diameter between the dentate and the edentulous group. The latter is confirmed by Mardinger et al. (2008), who detected a significant enlargement of the nasopalatine canal diameter by tooth loss. Iordanishvili (1991) found evidence of age- and gender-linked differences in the mean length of the nasopalatine canal using craniometric investigation on human skulls. This is in full agreement with the present observation on age and gender differences. Güler et al. (2005) reported that men had significantly bigger canals by measuring on panoramic radiographs, which could be confirmed in the present study. The present study allowed the nasopalatine canal and foramina to be determined using CT images from three dimensions. A careful assessment in three dimensions thus allowed for a better visualization of this critical anatomic structure, which could yield vital information during pre-surgical planning.

Currently, cone-beam CT imaging is preferred over traditional spiral CT for maxillofacial applications, considering the generation of a very low dose but high-quality image dataset (Loubele et al. 2008a, b).

Conclusions and Clinical Implications

The anatomical variability in morphology and dimensions of the nasopalatine canal together with the variability of the neurovascular content calls for awareness during clinical procedures in the maxillary central incisor region. This may be of clinical importance in administration of local anaesthesia, palatal surgery and implant surgery. An increased understanding of this anatomic structure could improve the success of surgery or avoid post-operative complications. A careful pre-operative planning using low-dose 3D imaging, such as with cone beam CT, is therefore recommended.

References

Artzi, Z., Nemcovsky, C. E., Bitlitum, I. & Segal, P. (2000) Displacement of the incisive foramen in conjunction with implant placement in the anterior maxilla without jeopardizing vitality of nasopalatine nerve and vessels: a novel surgical approach. *Clinical Oral Implants Research* **11**, 505–510.

Casado, P. L, Donner, M., Pascarelli, B., Derocy, C., Duarte, M. E. & Barboza, E. P. (2008) Immediate dental implant failure associated with nasopalatine duct cyst. *Implant Dentistry* **17**, 169–175.

Cavalcanti, M. G., Yang, J., Ruprecht, A. & Vannier, M. W. (1999) Accurate linear measurements in the anterior maxilla using orthoradially reformatted spiral computed tomography. *Dentomaxillofacial Radiology* **28**, 137–140.

Chandler, N. P. & Gray, A. (1996) Patent nasopalatine ducts: a case report. *The New Zealand Dental Journal* **92**, 80–82.

Daley, T. D., Wysocki, G. P. & Pringle, G. A. (1994) Relative incidence of odontogenic tumors and oral and jaw cysts in a Canadian population. *Oral Surgery, Oral Medicine, and Oral Pathology* **77**, 276–280.

Güler, A. U., Sumer, M., Sumer, P. & Biçer, I. (2005) The evaluation of vertical heights of maxillary and mandibular bones and the location of anatomic landmarks in panoramic radiographs of edentulous patients for implant dentistry. *Journal of Oral Rehabilitation* **32**, 741–746.

Haas, R., Mensdorff-Pouilly, N., Mailath, G. & Watzek, G. (1996) Survival of 1920 IMZ implants followed for up to 100 months. *International Journal of Oral and Maxillofacial Implants* **11**, 581–588.

Hassanali, J. & Mwaniki, D. (1984) Palatal analysis and osteology of the hard palate of the Kenyan African skulls. *The Anatomical Record* **209**, 273–280.

Higginbottom, F. L. & Wilson, T. G. Jr. (1996) Three-dimensional templates for placement of root-form dental implants: a technical note. *International Journal of Oral and Maxillofacial Implants* **11**, 787–793.

Iordanishvili, A. K. (1991) Age-related characteristics and sex differences in the anatomical structure of the incisive canal. *Stomatologiia* **71**, 25–27.

Jacob, S., Zelano, B., Gungor, A., Abbott, D., Naclerio, R. & McClintock, M. K. (2000) Location and gross morphology of the nasopalatine duct in human adults. *Archives of Otolaryngology – Head and Neck Surgery* **126**, 741–748.

Jacobs, R., Lambrichts, I., Liang, X., Martens, W., Mraiwa, N., Adriaensens, P. & Gelan, J. (2007) Neurovascularisation of the anterior jaw bones revisited using high resolution magnetic resonance imaging. *Oral Surgery, Oral Medicine, Oral Pathology, Oral Radiology, and Endodontics* **103**, 683–693.

Kraut, R. A. & Boyden, D. K. (1998) Location of incisive canal in relation to central incisor implants. *Implant Dentistry* **7**, 221–225.

Kreidler, J. F., Raubenheimer, E. J. & van Heerden, W. F. (1993) A retrospective analysis of 367 cystic lesions of the jaw – the Ulm experience. *Journal of Cranio-Maxillo-Facial Surgery* **21**, 339–341.

Loubele, M., Bogaerts, R., Van Dijck, E., Pauwels, R., Vanheusden, S., Suetens, P., Marchal, G., Sanderink, G. & Jacobs, R. (2008a) Comparison between effective radiation dose of CBCT and MSCT scanners for dentomaxillofacial applications. *European Journal of Radiology* **105**, 512–518. [Epub ahead of print].

Loubele, M., Van Assche, N., Carpentier, K., Maes, F., Jacobs, R., van Steenberghe, D. & Suetens, P. (2008b) Comparative localized linear accuracy of small-field cone-beam CT and multislice CT for alveolar bone measurements. *Oral Surgery Oral Medicine Oral Pathology Oral Radiology and Endodontics* **105**, 512–518.

Mardinger, O., Namani-Sadan, N., Chaushu, G. & Schwartz-Arad, D. (2008) Morphologic changes of the nasopalatine canal related to dental implantation: a radiologic study in different degrees of absorbed maxillae. *Journal of Periodontology* **79**, 1659–1662.

Moss, H. D., Hellstein, J. W. & Johnson, J. D. (2000) Endodontic considerations of the nasopalatine duct region. *Journal of Endodontics* **26**, 107–110.

Mraiwa, N., Jacobs, R., Van Cleynenbreugel, J., Sanderink, G., Schutyser, F., Suetens, P., van Steenberghe, D. & Quirynen, M. (2004) The nasopalatine canal revisited using 2D and 3D CT imaging. *Dentomaxillofacial Radiology* **33**, 396–402.

Radlanski, R. J., Emmerich, S. & Renz, H. (2004) Prenatal morphogenesis of the human incisive canal. *Anatomy and Embryology* **208**, 265–271.

Rosenquist, J. B. & Nyström, E. (1992) Occlusion of the incisal canal with bone chips. *Journal of Maxillofacial Surgery* **21**, 210–211.

Scher, E. L. (1994) Use of the incisive canal as a recipient site for root form implants: preliminary clinical reports. *Implant Dentistry* **3**, 38–41.

Sicher, H. (1962) Anatomy and oral pathology. *Oral Surgery, Oral Medicine, and Oral Pathology* **15**, 1264–1269.

Sicher, H. & DuBrul, E. L. (1975) *Oral Anatomy*, 6th edition. St. Louis: C. V. Mosby Company, p. 82, 345, 412, 438–439, 458.

Swanson, K. S., Kaugars, G. E. & Gunsolley, J. C. (1991) Nasopalatine duct cyst: an analysis of 334 cases. *Journal of Oral and Maxillofacial Surgery* **49**, 268–271.

Tolstunov, L. (2007) Implant zones of the jaws: implant location and related success rate. *Journal of Oral Implantology* **33**, 211–220.

White, S. C. & Pharoah, M. G. (2004) *Oral Radiography Principles and Interpretation*, 5th edition. St. Louis: C. V. Mosby Company, p. 174.

Address:
Xin Liang
Oral Imaging Centre
Faculty of Medicine
School of Dentistry
Oral Pathology and Maxillofacial Surgery
Catholic University of Leuven
Kapucijnenvoer 7
B-3000 Leuven
Belgium
E-mail: xin.liang@med.kuleuven.be

Clinical Relevance

Scientific rationale for the study: The use of implants in the maxillary incisor region has become part of routine dental practice. Yet, contact of implants with the fatty myelin content of nervous tissues of the nasopalatine canal may cause non-osseointegration of the implants and even lead to sensory dysfunction. The anatomic appearance and potential human variability of this canal remains however poorly documented.

Principal findings: HR-MRI and histological sections identified the nasopalatine canal containing a large artery surrounded by veins and myelinated nerves. Dimensional variation was substantial and a significant relation with age could be established, implying an increased size of the canal for elderly.

Practical implications: The present results imply that in order to avoid potential complications during surgery such as implant placement, surgeons should carefully inspect this region pre-operatively and avoid damaging the nasopalatine canal region. Low-dose 3D cone beam CT images are nowadays suitable for such analysis.